



Electrospun cellulose nanofibers from toilet paper

A. G. Kiper¹ · A. Özyuguran¹ · S. Yaman¹

Received: 7 March 2020 / Accepted: 16 July 2020 / Published online: 27 July 2020
© Springer Japan KK, part of Springer Nature 2020

Abstract

Toilet paper was used to produce cellulosic nanofibers through electrospinning method. Dissolution of toilet paper was attempted in either solutions of 0.5–8.5 wt% lithium chloride in Dimethylacetamide (LiCl/DMAc) or Trifluoroacetic acid (TFA). LiCl/DMAc solvent with concentrations lower than 8 wt% was incapable of completely dissolving the toilet paper even though several days of interaction. 8 wt% solvent dissolved the toilet paper, but the obtained solution was too viscous for spinning, and spraying occurred rather than spinning, and hardly visible deposits with fringed structure formed. In contrast, TFA solution dissolved the toilet paper, and the solutions could be spun easily. In these tests, spinning parameters were changed within the feeding rates of 2.00–9.25 mL/h, needle tip-to-collection plate distances of 140–205 mm, voltage of 23–28 kV, and relative humidity of 53–70%. The produced fibers were characterized by Scanning Electron Microscopy (SEM), X-ray Diffraction (XRD), and Fourier-Transform Infrared Spectroscopy (FTIR). It was concluded that the produced fibers are ultrafine with nanoscale diameter, and the morphologies of produced fibers are severely in the shape of bead-on-string fibers. Besides, the use of TFA solvent led to reduction in the crystallinity of cellulose that is one of the typical intrinsic characteristics of cellulose.

Keywords Nanofiber · Cellulose · Toilet paper · Electrospinning · Material cycles · Beads

Abbreviations

CA	Cellulose acetate
CrI	Crystallinity index
DMAc	Dimethylacetamide
FTIR	Fourier-Transform Infrared Spectroscopy
ILc	Ionic liquids
I_{\max}	Intensity maximum between $2\theta = 22^\circ$ and 23°
I_{\min}	Intensity minimum between $2\theta = 18^\circ$ and 19°
LiCl	Lithium chloride
SEM	Scanning Electron Microscopy
TFA	Trifluoroacetic acid
XRD	X-ray Diffraction

Introduction

Cellulose, that is a fascinating biopolymer, is regarded as the most important potential candidate to substitute the petroleum-based polymers due to various promising characteristics, such as sustainability, renewability, green nature, inexhaustibility, bio-degradability, bio-compatibility, high reinforcing potential, thermal and chemical stability [1]. Accordingly, investigations into nanofibers from cellulose have attracted great interest due to their outstanding properties that show high mechanical performance, large ratio of surface area to mass or volume due to small diameter, tunable porosity, and the diversity of surface functional groups [2,3]. Thus, natural fibers obtained from cellulose have widely been used in textile, biomedical, electronic, defense and security, materials, and environmental areas as non-woven fabrics, protecting clothing, wound dressing, tissue scaffolding, drug delivery systems, bandages, enzyme immobilization, electrically conductive fibers, photonic crystals, flexible photocells, biosensors, nano-fiber composites, reinforcement material, mineral processing, propellant applications, food package, paper making, biocatalysts, chemical synthesis, paints, plastics, pharmaceuticals, membranes, and cosmetics, etc. [1,3–14]. Recently, some

✉ S. Yaman
yamans@itu.edu.tr

¹ Chemical Engineering Department, Chemical and Metallurgical Engineering Faculty, Istanbul Technical University, 34469 Maslak, Istanbul, Turkey

high-technology sectors that include aerospace and nuclear engineering have also considered carbon nanofibers as cheap and environmentally friendly alternative of the materials in current use [15].

Electrospinning or electrostatic fiber spinning is a simple and efficient way to produce ultrathin- and continuous-polymer fibers in nanometer scale by the effect of an external electric field imposed on a polymer solution or melt [9,16]. The electric field converts a pendant droplet of the solution into conical shape that is called as *Taylor cone*, and once the applied electrical force at the interface of polymer solution overcomes the surface tension of the droplet, a fine charged jet is ejected and collected on a grounded electrode [9,17,18]. Three successive stages account for the electrospinning process. These stages are the formation of a Taylor cone, the straight fluid jet emitted from the Taylor cone, and the unstable region, which is composed of numerous bending and whipping loops [19]. Three groups of electrospinning parameters play critical role on formation of fibers and their morphology. These parameters are the process parameters (applied voltage, solution flow rate, needle tip-to-collection plate distance, and collector type), solution parameters (polymer concentration, surface tension, viscosity, conductivity, and polymer molecular weight), and ambient conditions (humidity and temperature) [9,11,17,20,21]. The viscosity of solution determines the range of concentration from which fibers can be obtained, and the surface tension is the dominant factor at low viscosities [21]. Increasing polymer concentration results in increasing diameters of fibers [9,16]. Also, when the distance from spinneret to collector is narrower than a definite opening, some beads and spots appear since the solvent is not completely evaporated because of short distance [9]. In opposite case, however, longer distances cause formation of thinner fibers [9]. Besides, the applied voltage is correlated with the formation of bead defects in the fibers [16]. The major advantage of this method is that nanofibers with diameter of 500 nm–2 μ m can be spun [6,12]. Non-woven textiles that are consisted of electrospun fibers have small pore size and large surface area, making them promising candidates for usage in filtration and membrane applications [16].

Electrospinning is not a new technique and it dates back to observations of Rayleigh in 1897, and the first patent (US Patent Number: 2116942) on electrospinning of fibers “Method and Apparatus for Production of Fibers” was issued in 1936 for the fabrication of textile yarns by electrospinning of cellulose acetate. Then, invention of electrical atomization method made it possible to form streams of highly electrified uniform droplets and liquids converted into aerosols under high electric field. But, the basic rules of electrospinning based on electrically driven jets were established by Taylor in 1969 [3]. The electrospinning method showed very rapid development over years and recent advances involved

new approaches to produce advanced functional nanomaterials via electrospinning.

Electrospun fibers have been tested in various applications and hundreds of studies performed recently in miscellaneous fields including multilayer nanofibrous membranes with antibacterial property for air filtration [22], bio-membrane for bone tissue applications [23], flexible capacitive sensor [24], scaffolds for controllable release of drugs [25,26], fibers for organic dye removal and antibacterial application [27], diffusion layers for direct methanol fuel cells [28], membranes for multicomponent wastewater treatment [29], architecture of high performance supercapacitors [30], etc.

It is reported that more than 200 polymers have been electrospun [3]. Of which, cellulose is of special interest in different fields of applications. In this context, some lignocellulosic feedstock has been attempted to obtain electrospun cellulose nanofibers. Namely, corn cellulose [6], durum wheat straw [31], rice straw [32], sugar cane straw [33], agricultural residue of coconut palm leaf sheath [34], cotton cellulose [7,12,35], indigo-dyed waste denim garments [36], softwood pulp [9], hardwood kraft pulps [37], cellulose from paper substrates [38], and lignocellulosic sisal [2] are among the materials tested in electrospinning. However, electrospun cellulosic fibers have mostly been fabricated using cellulose acetate (CA) solutions to which various chemicals were added so that the produced fibers have the desired properties according to their intended use. Hamad et al. [39] produced CA nanofibers impregnated with hydroxyapatite nanocomposite fibers for removal of heavy metals. Ojstrsek et al. [40] prepared electrospun nanofibrous composites from CA and ultra-high silica zeolites for adsorption of volatile organic compounds. Chen et al. [41] fabricated polyvinylidene fluoride/triphenyl phosphate/CA nanofiber membrane by one-step electrospinning and used it as separator in lithium-ion batteries. Tanvir et al. [42] fabricated nanoporous electrospun CA butyrate nanofibers for sorption of oil. Zhu et al. [43] synthesized a novel air filter made of CA and poly (ionic liquids) by electrospinning method. de Almedia et al. [44] used cationic surfactant to produce CA fibers with small diameters and with reduced bead formation. Araga et al. [45] synthesized amine functionalized electrospun cellulose nanofiber-based adsorbent from CA for removal of dissolved fluoride ions from groundwater.

Cellulose, which is a linear polysaccharide composed of β -(1 \rightarrow 4) linked glucose, shows high crystallinity supported by extensive hydrogen bonding network [46]. The inter- and intra-molecular hydrogen bonding among the molecules and the van der Waals forces between the non-polar groups make this cheap and abundant raw material undissolved in conventional organic and aqueous solvents [4–8]. An ideal solvent for electrospinning should have the requirements of (i) semi-conductivity with a moderate charge capacity, (ii)

high volatility for rapid solidification of fiber, and (iii) the ability to dissolve the polymer with minimum intermolecular interactions [12]. A number of different solvents have been tested to dissolve cellulose. However, most of the conventional cellulose solvents contain harmful/volatile substances that lead to environmental pollution and health concern [47]. Hence, novel solvents, such as DMAc (Dimethylacetamide)/LiCl, TFA (Trifluoroacetic acid), and various ionic liquids (ILs), have been developed to avoid this concern [6,7]. Room-temperature ILs are of great interest in electrospinning of cellulose, since they do not have pronounced vapor pressure and do not evaporate [7]. Of which, DMAc/LiCl, which is a solution of non-volatile salt (LiCl) in a volatile solvent (DMAc), is the most popular solvent [17]. This solvent that has low-toxicity is reported to be able to dissolve different cellulose types without serious degradation [6]. Interaction of the DMAc/LiCl solvent with cellulose occurs with the hydroxyl groups of cellulose via hydrogen bonding bridged by the chloride anion, and Li^+ interacts with the carbonyl oxygen via ion–dipole interaction. These interactions yield the soluble sulphonic acid esters, and the dissolution mechanism of cellulose in DMAc/LiCl is shown in Fig. 1 [48]. However, this dissolution mechanism in DMAc/LiCl is highly sensitive to the crystallinity of cellulose that obstructs the complete dissolution. Also, the solvent and the salt in cellulose should be completely removed after dissolution/regeneration [7]. Besides, the solution preparation can be challenging [8]. In addition, cellulose should be pre-activated by treatment of small molecular alcohols that improve the dissolubility of cellulose in DMAc/LiCl [6].

On the other hand, TFA, which is a very strong organofluorine acid, is able to dissolve cellulose at ambient temperature and can be easily eliminated from the cellulose solution by natural evaporation due to its low boiling point (72.4 °C) [2,7]. Dissolution of cellulose in TFA takes place by attack of TFA at glycosidic linkages. That is, TFA ($\text{pK}_a=0.23$) hydrolyzes polysaccharides better than even sulfuric acid and it preserves the monosaccharides produced during hydrolysis. The strong dissolution capability of TFA makes it an excellent solvent for cellulose even without pretreatment need of cellulose. Besides, the main challenge in the use of TFA arises from the strong acidic nature of TFA [7]. Nonetheless, Okhawa et al. [12] reported that TFA meets the requirements of (i), (ii), and (iii) for an ideal solvent

mentioned above, and can be regarded as the most suitable candidate for electrospinning of cellulose. Leyva et al. [31] produced cellulose nanofibers from wheat straw using TFA for which the polymer concentration changed in the range of 4–5.5 wt%. Also, Rodrigues et al. [2] electrospun lignocellulosic sisal fiber and sisal pulp from the solutions of TFA with concentrations of 0.02–0.03 g mL^{-1} at room temperature.

Although lots of lignocellulosic feedstocks including cotton, linen, ramie, sisal, and flax have been tried as raw material to produce carbon fibers [15], the isolation of cellulose from lignocellulosic materials through elimination of lignin and hemicellulose necessitates using of various potent chemicals [49,50]. In fact, cellulose, hemicellulose, and lignin that are the main macromolecular components of lignocelluloses are linked to each other with ether bonds [51], and the breakdown of these bonds needs effective thermal or chemical treatment. Since most of hemicellulose and lignin have already been separated from cellulose in paper fabrication process, their fractions are allowed to be very low compared to cellulose. Thus, paper products can be regarded as easy-to-find materials that are rich in celluloses [52]. Recycle of used paper products is one of the fundamental recycle applications regarding the benefits, such as it saves waste paper from occupying landfill where emits methane, saving the trees that will be otherwise cut for paper/pulp production, to lower water and energy consumption in paper production, etc. However, special types of papers and paperboards have their own recycle characteristics. Recycle of toilet paper is limited to the clean rejected toilet paper that cannot be put on the market because of manufacturing defects, improper packaging or swelling by water contact. Since toilet paper is highly rich in cellulose, the cellulosic fibers in these rejected toilet papers may be regarded as alternative source of cellulosic nanofiber production. In this way, an alternative source that is cheap and easy to use can be evaluated to produce high-grade and precious materials like cellulose nanofibers. In this context, using of paper products in manufacturing of cellulose fibers will avoid the expensive and time-consuming treatments to isolate cellulose from lignocellulosic feedstock. Scraps and rejected papers occurring during manufacturing, storage or transportation of paper may be directed to this new alternative utilization field. However, the paper products have rarely been attempted in nanofiber production yet, and only very little information is available on activation and dissolution of paper products in commonly used solvents relevant for spinning [38]. Yousef et al. [53] recently attempted to isolate cellulose from banknote production wastes to produce cellulose nanocrystals. However, the main challenge for this approach was the presence of metals in the banknote wastes originated from ink (Al, Fe, Ni, etc.) and metals from pigment (Si, Ti, etc.). Therefore, almost pure cellulosic papers like toilet paper may offer special opportunity for such applications. In this context, the

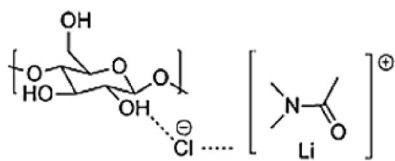


Fig. 1 Dissolution mechanism of cellulose in DMAc/LiCl solvent

novelty of this paper lies on the use of cellulosic toilet paper for manufacturing of the carbon nanofibers by electrospinning technique. In this way, a new and alternative method will be proposed for recycling of rejected toilet paper to produce cellulosic nanofibers that are of great interest in scientific, medical, and technological applications.

Materials and methods

Materials

Toilet paper used in this study was provided from a local Turkish company, and it was pure cellulosic product. Alpha (α)-cellulose, which has the highest degree of polymerization and the most stable kind of three classes of cellulose forms (α , β , γ), accounts for almost all of the toilet paper structure. The chemical composition of toilet paper can be given by $(C_6H_{10.9}O_{5.3})_n$ that is highly comparable with that of pure cellulose $(C_6H_{10}O_5)_n$ [54].

The toilet paper was cut into small pieces (10 × 10 mm sizes) with a scissors, and was kept in a Petri dish before use. The chemicals used in dissolution and activation experiments are LiCl (Sigma, $\geq 99\%$), DMAc (Merck, $\geq 99.5\%$), Acetone (Sigma, $\geq 99.5\%$), TFA (Carlo Erba, 98% and Merck, 99%), cellulose acetate (Sigma, 98%), and methanol (Merck, 99.5%). All of these chemicals were used at the mentioned concentrations without any further enrichment.

Methods

Nanospinner24-XP electrospinning apparatus with upward spinning nozzle that avoids trickle of the droplet was used. Owing to the multiple nozzles, this apparatus enables formation of great deal of fibers relatively in short times. In addition, nanofibers with versatile thickness can be produced through the horizontally moving collector. The needle tip-to-collection plate distance is adjustable, and the ambient temperature and the humidity are seen on the display.

To test the spinning ability of the electrospinning device, the solution of cellulose acetate (CA) was first spun in this device as a reference material. Although it is known that the solubility properties of CA ($C_{164}H_{174}O_{111}$) and cellulose differ seriously, this experiment was performed only to check the spinning performance of the device to be used in the spinning of cellulose in toilet paper. CA used in this test has an average molecular weight (M_n) of about 30,000 and the degree of acetyl substitution is around 2.4. The solution of CA-Acetone-DMAc was prepared and electrospun. For this purpose, acetone and DMAc in 2/1 vol. ratio were mixed for 1 h by magnetic stirrer, and then CA in different concentrations (15, 17, and 20 vol%) was added to the solution.

The resulting mixture was stirred for additional 2 h prior to electrospinning.

Electrospinning of cellulose from toilet paper was attempted using two alternative solvents. In the former, LiCl in DMAc solutions (0.5–8.5 wt%) was used to dissolve the pieces of pre-activated toilet paper with water, methanol and DMAc, while in the latter, TFA was used without any pre-activation. 0.5, 0.8, 1, 1.2, 1.25, 1.5, 1.8, 2, 4, 6, 8 and 8.5 wt% LiCl containing LiCl/DMAc solutions was prepared. For an instance, to prepare 8 wt% LiCl/DMAc solution, 0.8 g anhydrous LiCl was added to 9.2 g DMAc solution, and the mixture was stirred by magnetic stirrer. In these experiments, the concentration of cellulose in solutions was changed between 0.5–3.0 wt%. The pre-activation of cellulose was performed based on the polar-medium-exchange approach by treatment with water (30–60 min × 2 times), methanol (30–60 min × 2 times), and DMAc (30 min and overnight). Vacuum filtration was employed after each treatment to dry out the treated bulk. Then, the pre-activated cellulose was mixed with LiCl/DMAc solvents. This mixture was kept stirred for at least two days to facilitate the complete dissolution of cellulose. The concentration of cellulose in TFA solvent was changed in the range of 2.00–2.75 wt% since concentrations lower than 2 wt% did not yield fibers. Also, the solutions were heated to 60 °C before electrospinning.

Effects of the parameters relevant in electrospinning process were investigated within the feeding rates of 2.00–9.25 mL/h, distances of 140–205 mm between syringe and collector, voltage of 23–28 kV, and the relative humidity of 53–70%. Also, the influence of leaving the nanofibers to rest under ambient air condition was also studied. For this purpose, nanofibers spun using TFA solvent were rested at ambient temperature for three days to get dried fibers where TFA evaporated. Conversely, fibers that will be named hereafter as “Nanofiber2” were not rested under air, and accordingly its contact with air is highly limited. On the other hand, the solution that contains toilet paper and TFA was poured onto a glass plate where it was allowed to dry out. The specimen obtained in this way will be named henceforth as “cast film”.

Characterization of the produced nanofibers, cast film, and untreated toilet paper was carried out by Scanning Electron Microscopy (SEM), Fourier-Transform Infrared Spectroscopy (FTIR), and X-ray Diffraction (XRD) techniques. The morphology of the samples was investigated by SEM images obtained using Quanta 250 FEG device (Thermo Fisher Scientific Company) with a magnification ratio of up to $10^6\times$ and up to 4096×3536 pixels (~ 14 MP). Prior to analysis, the samples were coated with thin film of platinum by Quorum Technologies Ltd SC7620 mini sputter coater. FTIR spectra were obtained using Spectrum 100 model FTIR instrument manufactured by Perkin Elmer that gives data over a total range of 7800 to 370 cm^{-1} to specify the

surface functionalities and the main functional groups in samples blended with KBr. XRD technique was employed to check the crystallinity of cellulose by PANalytical X'Pert Pro model device of Panalytical Company powered by a Philips PW3040/60 X-ray generator. X-rays were generated from a Cu anode supplied with 45 kV and a current of 40 mA.

Results and discussion

Electrospinning of cellulose acetate (CA)

To check the performance of the electrospinning device to produce smooth cellulosic fibers, the solutions of CA in acetone and DMAc were subjected to electrospinning conditions as reference test. Cellulosic fibers were produced successfully, and Table 1 presents the conditions applied during these tests. SEM images of the fibers showed that quite smooth fibers could be obtained and as the concentration of the solution increased, the fibers tended to thicken. SEM image of the fibers obtained from CA solution with 17 vol% concentration of CA is shown in Fig. 2. This image demonstrates that the electrospinning device operates satisfactorily, and smooth fibers can be generated. The average diameter of cellulose fibers was measured as 126.9 ± 12 nm that shows the obtained fibers are almost uniform and their diameters change in a narrow interval. The morphology of the electrospun fibers is highly consistent with the findings of Son et al. [55] within the similar CA concentration range. When solution concentration increased to 20 vol%, mean diameters of the fibers were around 400 nm with the minimum and maximum diameters of 200 nm and 537 nm, respectively. On the other hand, dissolution of CA using only DMAc (without acetone) was also tested. However, smooth fibers could not be produced in this case by electrospinning.

Dissolution of toilet paper in LiCl/DMAc solvent

It was aimed to prepare paper solutions with concentrations of 0.5–3.0 wt% using 0.5–8.5 wt% LiCl/DMAc solvents. Visual inspections for the extent of dissolution of

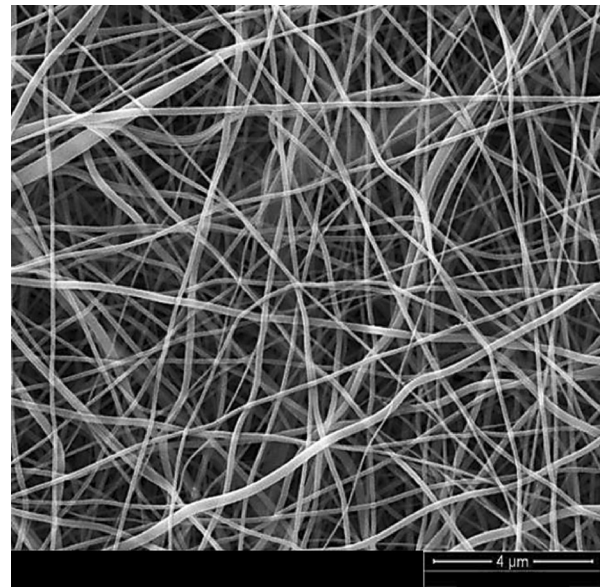


Fig. 2 SEM image of 17 vol% CA in Acetone-DMAc

2 wt% paper in 2, 4, 6, and 8 wt% LiCl/DMAc solutions are shown in Fig. 3.

Dissolution of paper in the solutions of 0.5–6 wt% LiCl/DMAc failed since the complete dissolution did not take place although several days of interaction periods were allowed. Despite the applied pretreatment (activation), LiCl/DMAc with concentrations lower than 8 wt% was incapable of complete dissolution of cellulose probably due to the crystal nature of cellulose which was not wholly destroyed. Insufficient disruption of hydrogen bonding between chains might lead to lack of complete dissolution of cellulose when the concentration was less than 8 wt%. This is in agreement with earlier works that address the difficulty of dissolution of cellulose in such solvents [38,56]. The NMR analysis on cellulose acetate (CA) dissolution pointed out in these studies that interaction of DMAc solvent molecule with O–Ac group or OH group in CA was less than that of TFA solvent molecule. Besides, it has been widely reported that the dissolution of cellulosic materials in LiCl/DMAc solutions is time-consuming and often leads to swelling of cellulose. In addition, the type of the precursor of cellulose may also affect the performance of the solvent used. Namely, hardwood kraft pulps have been reported to be completely dissolved in LiCl/DMAc solutions, whereas softwood pulps may have a limited solubility [37]. Manufacturers of toilet paper generally use a combination of softwood (30 wt%) and hardwood (70 wt%) trees. The softwood fraction may also play a negative role on the dissolution of cellulose. Pretreatment of cellulose with water, methanol and DMAc did not improve the dissolubility of cellulose.

Table 1 Conditions for electrospinning of CA

Concentration (vol%)	Flow rate (mL/h)	Distance (mm)	Voltage (kV)	Rel. hum (%)	Temperature (°C)
15	1.00	170	19	46	24
17	0.70	170	19	61	22
20	0.55	160	19	55	23

CA Cellulose acetate, Rel.Hum. Relative humidity

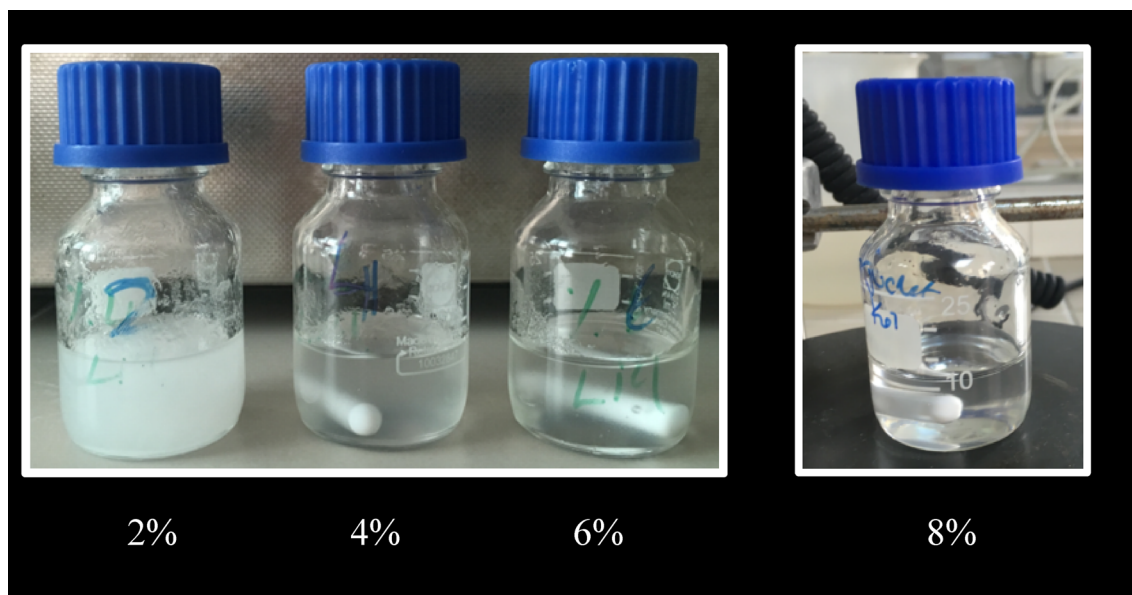


Fig. 3 Dissolution of 2 wt% toilet paper in LiCl/DMAc solutions

On the contrary, the treatment with 8 wt% LiCl/DMAc resulted in complete dissolution of cellulose, and the obtained solution was used in the electrospinning test. Unfortunately, smooth fibers could not be obtained using this solution since it was too viscous to spin. It is known that the electrorheological properties and the viscosity of solution at the ejection point play critical role in electrospinning. The molecular weight of the dissolved polymer determines the viscosity of solution. Considering the molecular weight of cellulose, it is not so surprising to see that the solution is highly viscous. Barhoum and Makhoulouf [57] also reported a similar situation where interactions of lignin and some chemicals increased the viscosity. Too high viscosity made the solution very difficult to pump through the syringe needle. Also, highly viscous solution may dry at tip of the needle before the start of electrospinning. In contrast to this, when the solution viscosity is not too high, there may be secondary jet erupting from the main electrospinning jet that leads to the formation of very thin fibers. The mentioned secondary effect that contributes to the formation of fibers could not be observed because of high viscosity. To overcome this concern due to high viscosity, some measures were taken including the heating of the solution in a water bath or using a heat gun just before spinning. Li et al. [35] also tried to heat the pathway between the tip of the needle and the collector. However, these measures did not work properly to yield smooth fibers. That is, solution was sprayed rather than spinning, and hardly visible deposits with fringed structure formed. It is known that both the solution viscosity and the electrical properties determine the extent of elongation of the solution [58]. The viscosity of the polymer

solution has significant influence in electrospinning process and the resultant fiber morphology. Thus, no smooth fibers could be obtained under the investigated conditions. Further investigation must be conducted by measuring viscosity, zeta potential, rheological properties, viscoelastic properties, and diffusion coefficient at different temperatures to estimate the optimum conditions for electrospinning. Nevertheless, the conditions of 0.4–0.9 mL/h of feeding rate, 25 kV of voltage, 120 mm distance, 30–32 °C of temperature, and 44–64% relative humidity gave relatively a bit more hopeful results and can be considered as a base for further investigations. Also, aside from methanol, other polar solvents should be tried to activate the cellulose in toilet paper.

Dissolution of toilet paper in TFA solvent

In the second part of the dissolution experiments, the solvent was shifted from LiCl/DMAc to TFA. For this purpose, the pieces of paper were interacted with TFA solvent at ambient temperature for several days while stirring by magnetic stirrer. In this way, very clear cellulose solutions with concentrations of 2.00–2.75 wt% were prepared and used in electrospinning experiments. The tested conditions for electrospinning of paper in TFA are given in Table 2. The conditions of these tests are almost comparable with those published in literature [31]. Cellulose fibers could be obtained more or less in similar characteristics under investigated conditions of solution concentrations, flow rates, distances, voltages, and relative humidity values. Among these parameters, the solution concentration was seen as the most dominant parameter that affects the thickness and the

Table 2 Electrospinning conditions using TFA solvent

Conc (wt%)	Flow rate (mL/h)	Distance (mm)	Voltage (kV)	Relative humidity (%)	Temp
2.0	5	160	27	55	Ambient
2.6	5	160	27	70	Ambient
2.5	5	160	27	61	Ambient
2.5	5	180	27	61	Ambient
2.5	5	190	27	61	Ambient
2.5	5	200	27	61	Ambient
2.5	5	180	27	60	Ambient
2.5	5	170	27	60	Ambient
2.5	5	190	27	64	Ambient
2.5	5	205	27	59	Ambient
2.5	5	160	27	60	Ambient
2.5	5	190	27	60	Ambient
2.5	4	170	27	60	Ambient
2.5	7	180	27	60	Ambient
2.5	2	140	27	53	Ambient
2.5	2.5	150	23	53	Ambient
2.5	2.25	150	26	53	Ambient
2.37	5	170	26	53	Ambient
2.37	9.25	180	27	53	Ambient
2.75	7.25	180	28	57	Ambient
2.5	5	160	27	56	Ambient

smoothness of the fibers. Therefore, following interpretations based on the effects of solution concentration on fiber properties, it was also observed that the viscosity of these solutions was explicitly lower than that for the LiCl/DMAc solvent. On the other hand, it is also known that TFA solvent is able to dissolve not only cellulose, but also hemicellulose and lignin to some extent if they are co-existing in paper in trace amounts [2]. This means that the use of TFA solvent offers a significant advantage over LiCl/DMAc when paper-derived materials are utilized. The obtained solution was poured onto a glass Petri dish and cured at the ambient condition. To ensure the complete removal of the solvent, the cast film was also further dried for three days. Electrospinning of these solutions was implemented successfully, and the distributions of the fiber diameters are given in Fig. 4. The mean diameter of fibers obtained from the solution of 2 wt% paper was 209 nm with the minimum and maximum diameter values of 55 nm and 358 nm, respectively. This shows that the mean diameter exceeds the benchmark value of 100 nm for being nanofiber. Increasing the paper concentration to 2.5 wt% resulted in significant decrease in the fiber diameter, and the mean diameter reduced to 40.6 nm with the minimum and maximum diameters of 16.7 nm and 68 nm, respectively, indicating that all of fibers are in nanofiber size. However, further increase in concentration to 2.75 wt% led to some enlargement in diameter, and the mean diameter enhanced to 91.3 nm with the minimum and

maximum values of 20 nm and 200 nm, respectively. The lower limits of fiber diameter intervals for 2.5 wt% and 2.75 wt% are almost comparable (16.7 nm and 20 nm, respectively). However, the upper limits of the fiber diameter intervals differed substantially from each other (68 nm and 200 nm). This is convenient with the results in literature reporting that the increasing concentrations favor the formation of fibers with increasing diameter, and consequently not nano-scaled fibers which are rather in helix-shaped micro-ribbons form [9,16]. This indicates that the concentration of 2.5 wt% is the optimum concentration for electrospinning of paper in TFA solvent. Rodrigues et al. [2] also prepared solutions with concentration of 2×10^{-2} g/mL by dissolving untreated lignocellulosic sisal fiber in TFA, and determined that the diameter of electrospun fibers ranged between 120 and 510 nm. On the other hand, the optimum solution conditions for other studies in literature where TFA solvent was used were usually a bit higher than our findings. Leyva et al. [31], who electrospun the durum wheat straw cellulose with solution concentrations of 4–5.5 wt% using TFA, reported nanofiber diameter range of 270 ± 97 nm. Also, Ohkawa et al. [12] addressed diameters changing between 60 and 75 nm for electrospun fibers from 4.5 wt% solution of cotton cellulose.

Effects of other parameters, such as the flow (feeding) rate, distance, voltage, and humidity, on fiber morphology were also investigated keeping the solution concentration

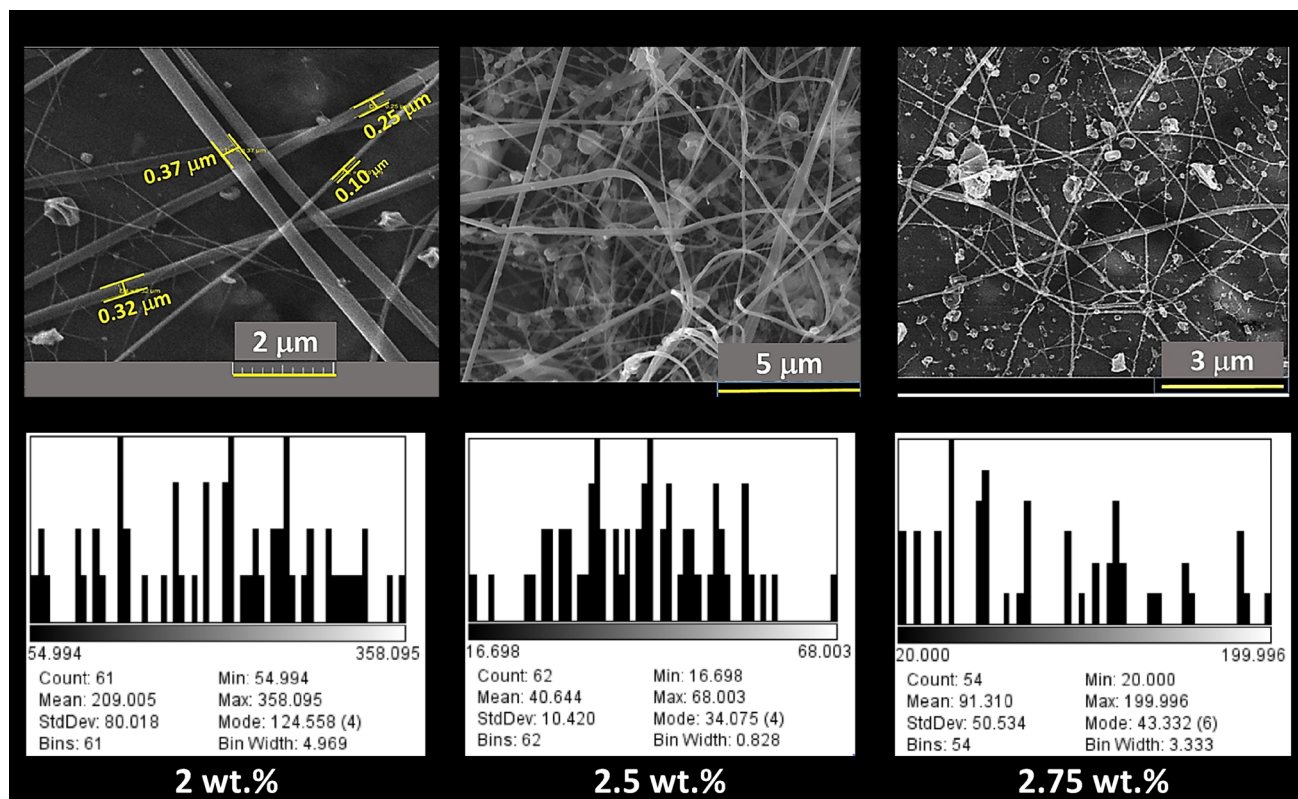


Fig. 4 SEM images and distribution of fiber diameters in nanometer

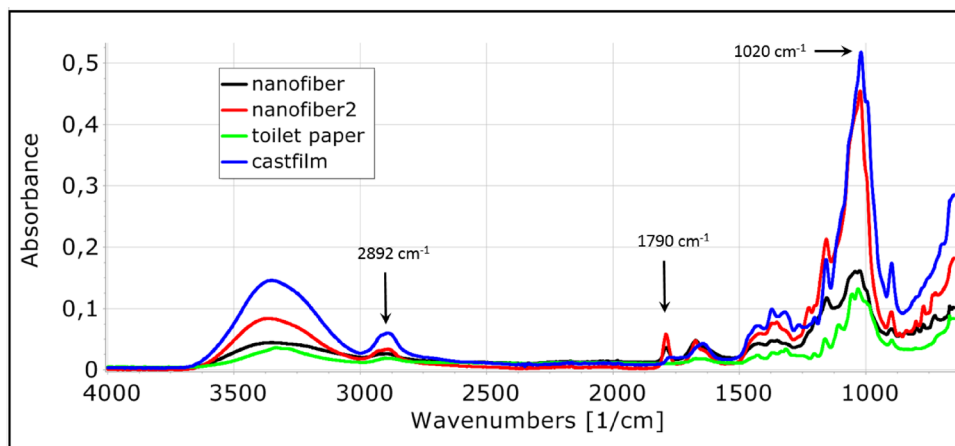
at 2.5 wt%. Any increase in flow rate from 2 up to 7 mL/h resulted in formation of relatively thicker fibers with larger beads. This situation can be linked with the fact that as the flow rate increased, the jet had less evaporation time before reaching the collector. In addition, the fibers seemed tend to get adhesion that increased the diameter [35]. The effect of voltage was tested in the range of 23,000–28,000 V. The voltage value of 27,000 V was previously seen as optimum voltage, and the effects of changes in voltage around this value were commented. That is, decrease in voltage impaired the fiber formation potential since electrostatic forces had difficulty to overcome the surface tension, while the increase in voltage led to formation of fibers that contain large beads. The distance between the needle tip-to-collection plate was changed between 140 and 205 mm. The distance of 160 mm was found optimum, and any increase or decrease in this distance enhanced the formation of bead-on-string fibers. The beads and spots that appeared when distance was shorter can be attributed to the incomplete evaporation of the solvent as reported by Awal et al. [9]. On the other hand, longer distances associated with longer stretching time led to formation of very tiny fibers. Similarly, Ohkawa et al. [12] concluded that 150 mm was the optimum distance for preparation of pure cellulose nanofibers via electrospinning. The effects of relative humidity in medium may also affect

the electrospinning characteristics of a polymer depending on its hydrophobic or hydrophilic properties. Therefore, the relative humidity during the experiments was recorded, and its effects on fiber morphology were observed. In this context, we determined that the relative humidity of 50–60% was optimum for electrospinning.

Characterization of electrospun fibers

FTIR spectroscopy was used to reveal the characteristic peaks in the samples, and Fig. 5 illustrates the FTIR spectra of nanofiber, nanofiber2, untreated toilet paper, and cast film. In general, the FTIR spectra bands are highly consistent with the bands of pure cellulose given in literature [59]. That is, the bands in this polysaccharide at around 1020 and 2892 cm^{-1} are typical bands that represent the presence of C–O and C–H bonds, respectively [60]. Likewise, the region of 2800–3600 cm^{-1} denotes O–H bonds. Comparison of the FTIR spectra of nanofibers (nanofiber and nanofiber2) with that of the toilet paper indicated some structural changes that can be attributed to the dissolution and electrospinning steps. That is, the absorption band around 1020 cm^{-1} originated from the presence of C–O bonds of cellulose became more evident in nanofibers. Leyva et al. [31] attributed such changes to breaking of the fibrillary structure as

Fig. 5 FTIR spectra



a consequence of dissolution in TFA, and formation of new groups, such as trifluoroacetyl esters. This observation is also consistent with the absorption band at 1790 cm^{-1} that predicts the existence of carbonyls of the trifluoroacetyl ester groups [2,31]. It is also reported that the degree of substitution of these groups decreases as the solution is exposed to air. Hydrolyzation by moisture in air facilitates the natural evaporation of the solvent. Accordingly, the intensities of the bands at 1790 cm^{-1} for cast film are seriously reduced in comparison to the nanofibers. Besides, the highest intensity at this band belonged to nanofiber2 where the exposure of this fiber to air is shorter than nanofiber or cast film. This indicates that exposure of the dissolved cellulose to air led to evaporation of TFA solvent. Removal of the solvent is highly vital especially in food packaging and textile applications.

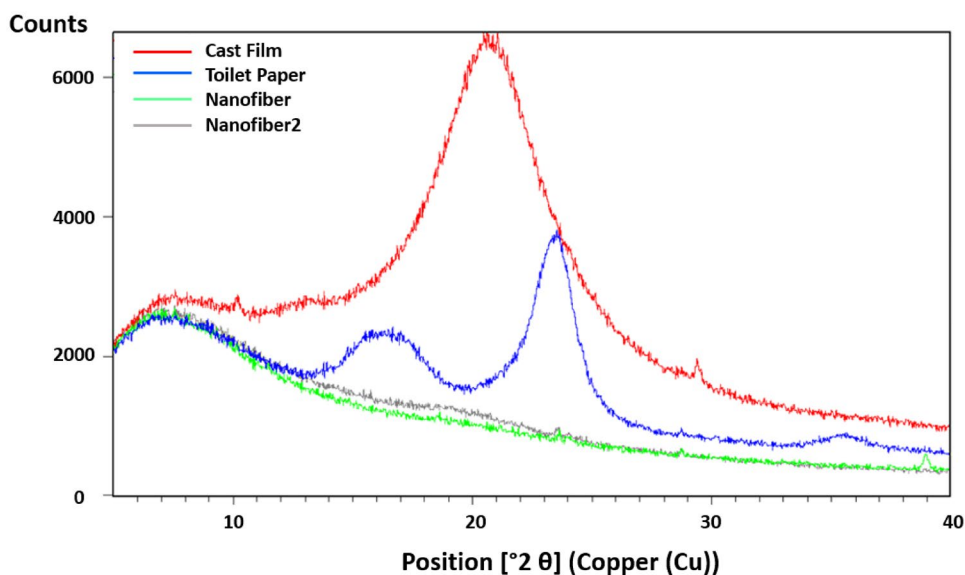
XRD spectra of the samples are shown in Fig. 6. The crystallinity of cellulose can be identified based on XRD spectra [21,31,34,61–65]. In this context, some approaches

have been proposed to quantify the cellulose crystallinity [34,63,65]. Following equation can be used to calculate the crystallinity index of cellulose [65]:

$$\text{CrI} = 1 - \frac{I_{\min}}{I_{\max}} \quad (1)$$

where, CrI is the crystallinity index, I_{\min} denotes the intensity minimum between $2\theta = 18^\circ$ and 19° , while I_{\max} means the intensity of the crystalline peak at the maximum between $2\theta = 22^\circ$ and 23° . CrI was calculated as 54% for untreated toilet paper, and this value is comparable with some results in literature. Maheswari et al. [34] found the crystallinity index of cellulose extracted from coconut palm leaf sheath to be 47.7%. Leyva et al. [31] found fiber's crystallinity 62%, and cellulose from rice straw fibers is reported to have the 63% crystallinity [32]. Dissolution of toilet paper in TFA solvent seriously lowered the

Fig. 6 XRD spectra



crystallinity index, and CrI value for cast film decreased to 35.1%. It is known that the crystalline system of cellulose is affected from both chemical and mechanical treatments [21,31]. Disruption of hydrogen bonds between cellulose chains by treatment leads to lower crystallinity compared to raw cellulose [21]. Besides, electrospinning is also reported to reduce the crystallinity [31]. However, the crystallinity could not be determined for the nanofibers by this approach since there were not any marked differences in the diffraction intensities. Similarly, He et al. [61], who fabricated cellulose nanofibers by electrospinning of cotton cellulose using LiCl/DMAc solution, also reported almost amorphous structure of electrospun fibers based on XRD data. However, the crystalline nature of fibers is one of the properties that define the mechanical properties [9]. From this point of view, it may be regarded that the tensile properties of the produced nanofibers are relatively low. On the other hand, the amorphous nature of fibers may be beneficial for rapid biodegradation.

The morphology of the cellulose fibers was analyzed by SEM images, and Fig. 7a shows the SEM image of the electrospun fibers obtained from 2.5% concentration solution using TFA. The parameters of feeding rate, distance, voltage, and humidity were 5 mL/h, 160 mm, 27 kV, and 56%, respectively. The diameters of the labeled fibers on this image demonstrate the existence of ultrathin fibers with nanoscale diameters, and this is similar with the findings of Santos et al. [1]. In addition, this image also reveals the fact that some beads formed on the fibers. The microstructure of the beads can be better seen in Fig. 7b by changing the magnification ratio of the image. Likewise, other working conditions given in Table 2 also resulted in formation of similar beads.

Although smooth fibers are the desired product in most of the electrospinning processes [66], formation of beads is often observed, and the instability of the polymer solution jet governs this phenomenon [17]. On the other hand, some factors, such as solution viscosity, surface tension, and net charge density, affect the formation of beads [67,68]. Gelation is also regarded as another possible factor that leads to formation of beads when the boiling point of the solvent is low [8]. Also, low concentrations of polymer solution may favor formation of beads [67]. Ohkawa et al. [12], who investigated effects of TFA concentration (2–5 wt%) on the morphologies of electrospun cellulose fibers from cotton and wood pulp, concluded that beads-free electrospun fibers could be obtained only in case of the highest concentration. However, high concentrations also result in high viscosity, which made the spinning very difficult in our experiments. In contrast to this, Fong et al. [68] showed the beneficial effect of high viscosities to avoid formation of bead. On the other hand, it is also reported that when the distance between spinneret and collector is narrow, some beads and spots may form due to incomplete evaporation of solvent. However, the mentioned distances in literature are well below than 160 mm that was implemented in our study [9]. Another important aspect is seen in distribution of the beads throughout the fiber structure. It is also known that the bead diameter and spacing are related to the fiber diameter, and in case of thin fibers, the distances between the beads are relatively short [68].

Beads on the fibers are usually regarded as a defect for electrospun fibers, and hence the spinning conditions are optimized to avoid formation of the beads. Nevertheless, the presence of beads may exhibit unique properties that

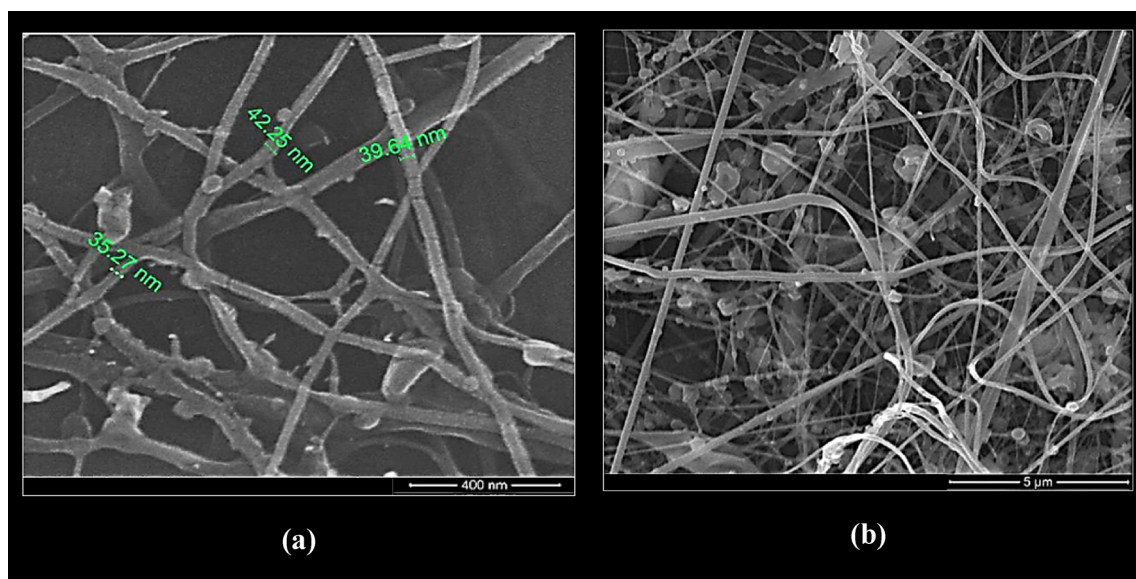


Fig. 7 SEM image of the nanofibers

benefit specific applications. Recent investigations indicated that the bead-on-string fibers have interesting benefits in many fields, such as tissue engineering, drug delivery, and air/water filtration [69]. Beads, in micron size, are able to carry high doses of drug in the tissue engineering scaffolds, and they are highly effective for drug-loading and sustained drug-releasing purposes [70]. Therefore, it is reported that the presence of these spheres seriously increases the drug-carrier performance of electrospun fibers that are too fine to incorporate high doses of drug. In addition to this, the microporosity in bead-on-string fibers also enhances air/water filtering performance of electrospun fiber filters [71]. The filtration efficiency of traditional non-woven fiber materials is relatively low for fine particles. Fibers that are rich in beads covered with micropores improve the packing density and facilitate air flow and adsorption for solid particles in air [72]. In addition, smooth nanofibers utilized in sensors and microelectronics often face practical difficulty in establishing proper contact between the probe and the fiber, and beads offer a much bigger target for contact with the probe [73]. For these reasons, the obtained fibers should be further investigated to justify their real performances in such specific applications.

This study showed that recycle of very cheap and abundant cellulosic toilet papers in an alternative manner using electrospinning method is able to produce cellulosic nanofibers that can be utilized in very different application areas.

Conclusion

Toilet paper was used in this study as an alternative material to fabricate the electrospun nanofibers of cellulose. This material that is highly rich in cellulose does not require the isolation step of cellulose from lignin and hemicellulose that are unavoidable accompanying macromolecules of cellulose in lignocelluloses. Dissolubility of the toilet paper pieces in either LiCl/DMAc or TFA solvents showed different dissolution characteristics. It was determined that LiCl/DMAc solvent did not solve cellulose when its concentration was lower than 8 wt%. In contrast to this, LiCl/DMAc at concentration bigger than 8 wt% was able to dissolve cellulose thoroughly. However, high viscosity of the solution led to serious difficulty in spinning, and smooth fibers could not be obtained. In contrast to this, TFA solvent was seen highly efficient to dissolve the toilet paper, and very clear solutions of cellulose were prepared. Besides, the treatment with TFA also reduced the cellulose crystallinity. The solutions of cellulose with TFA could be spun easily to produce cellulose fibers. Paper concentration of 2.5 wt% in TFA was allowed as optimum concentration for electrospinning. SEM images of the produced fibers predicted that they were ultrafine with diameters starting from 17 to 20 nm. However, it was seen

that the produced fibers are highly rich in beads. Although, fibers containing beads are mostly regarded as poor quality fibers, some specific applications, such as drug delivery or separation, may take advantage of this characteristics of the fibers. Thus, further investigations should be implemented on these specific areas to reveal the effectiveness of beaded fibers. It can be concluded that rejected toilet paper can be reused by converting it into more valuable technological products, such as nano-sized carbon fiber, and electrospinning method was seen as a promising method to recycle these cellulosic materials.

Acknowledgement This work was financially supported by the Scientific Research Projects (BAP) Unit of Istanbul Technical University (Project number: MYL-2018-41504). Also, the authors would like to thank Aysen Akturk (MSc) for her helps.

References

1. Santos RPO, Rodrigues BVM, Ramires EC, Ruvolo-Filho AC, Frollini EC (2015) Bio-based materials from the electrospinning of lignocellulosic sisal fibers and recycled PET. *Ind Crops Prod* 72:69–76. <https://doi.org/10.1016/j.indcrop.2015.01.024>
2. Rodrigues BVM, Ramires EC, Santos RPO, Frollini E (2014) Ultrathin and nanofibers via room temperature electrospinning from trifluoroacetic acid solutions of untreated lignocellulosic sisal fiber or sisal pulp. *J Appl Polym Sci* 41826:1–8. <https://doi.org/10.1002/APP.41826>
3. Bhardwaj N, Kundu S (2010) Electrospinning: a fascinating fiber fabrication technique. *Biotechnol Adv* 28:325–347. <https://doi.org/10.1016/j.biotechadv.2010.01.004>
4. Viswanathan G, Murugesan S, Pushparaj V, Nalamasu O, Ajayan PM, Linhardt RJ (2006) Preparation of biopolymer fibers by electrospinning from room temperature ionic liquids. *Biomacromol* 7:415–418. <https://doi.org/10.1021/bm050837s>
5. Ahn Y, Lee SH, Kim HJ, Yang YH, Hong JH, Kim YH, Kim H (2012) Electrospinning of lignocellulosic biomass using ionic liquid. *Carbohydr Polym* 88:395–398. <https://doi.org/10.1016/j.carbpol.2011.12.016>
6. Chen H, Ni J, Chen J, Xue W, Wang J, Na H, Zhu J (2015) Activation of corn cellulose with alcohols to improve its dissolvability in fabricating ultrafine fibers via electrospinning. *Carbohydr Polym* 123:174–179. <https://doi.org/10.1016/j.carbpol.2015.01.023>
7. Mahadeva SK, Yang SY, Kim J (2013) Effects of solvent systems on its structure, properties and electromechanical behavior of cellulose electro-active paper. *Curr Org Chem* 17:83–88. <https://doi.org/10.2174/138527213805289114>
8. Schiffman JD, Schauer CL (2008) A review: electrospinning of biopolymer nanofibers and their applications. *Polym Rev* 48:317–352. <https://doi.org/10.1080/15583720802022182>
9. Awal A, Sain M, Chowdhury M (2011) Preparation of cellulose-based nano-composite fibers by electrospinning and understanding the effect of processing parameters. *Compos B* 42:1220–1225. <https://doi.org/10.1016/j.compositesb.2011.02.011>
10. Greiner A, Wendorff JH (2007) Electrospinning: a fascinating method for the preparation of ultrathin fibers. *Angew Chem Int Ed* 46:5670–5703. <https://doi.org/10.1002/anie.200604646>
11. Hardelin L, Thunberg J, Perzon E, Westman G, Walkenström P, Gatenholm P (2012) Electrospinning of cellulose nanofibers from ionic liquids: the effect of different cosolvents. *J Appl Polym Sci* 125:1901–1909. <https://doi.org/10.1002/app.36323>

12. Ohkawa K, Hayashi S, Nishida A, Yamamoto H (2009) Preparation of pure cellulose nanofiber via electrospinning. *Text Res J* 79:1396–1401. <https://doi.org/10.1177/0040517508101455>
13. Naqvi SR, Mysore Prabhakara H, Bramer EA, Dierkes W, Akkremman R, Brem G (2018) A critical review on recycling of end-of-life carbon fibre/glass fibre reinforced composites waste using pyrolysis towards a circular economy. *Resour Conserv Recy* 136:118–129. <https://doi.org/10.1016/j.resco.2018.04.013>
14. Na O, Xi YP (2017) Mechanical and durability properties of insulation mortar with rubber powder from waste tires. *J Mater Cycles Waste Manage* 19:763–773. <https://doi.org/10.1007/s10163-016-0475-2>
15. Chand S (2000) Review—Carbon fibers for composites. *J Mater Sci* 35:1303–1313. <https://doi.org/10.1023/A:1004780301489>
16. Deitzel JM, Kleinmeyer J, Harris D, Tan NCB (2001) The effect of processing variables on the morphology of electrospun nanofibers and textiles. *Polymers* 42:261–272. [https://doi.org/10.1016/S0032-3861\(00\)00250-0](https://doi.org/10.1016/S0032-3861(00)00250-0)
17. Frey MW (2008) Electrospinning cellulose and cellulose derivatives. *Polym Rev* 48:378–391. <https://doi.org/10.1080/15583720802022281>
18. Kim CW, Frey MW, Marquez M, Joo YL (2005) Preparation of submicron-scale, electrospun cellulose fibers via direct dissolution. *J Polym Sci Part B Polym Phys* 43:1673–1683. <https://doi.org/10.1002/polb.20475>
19. Wang M, Hai T, Feng Z, Yu DG, Yang Y, Bligh SWA (2019) The Relationships between the working fluids, process characteristics and products from the modified coaxial electrospinning of Zein. *Polymers* 11:1287. <https://doi.org/10.3390/polym11081287>
20. Sukigara S, Gandhi M, Ayutsede J, Micklus M, Ko F (2003) Regeneration of Bombyx mori silk by electrospinning—part 1: processing parameters and geometric properties. *Polym* 44:5721–5727. [https://doi.org/10.1016/S0032-3861\(03\)00532-9](https://doi.org/10.1016/S0032-3861(03)00532-9)
21. Son WK, Youk JH, Park WH (2004) Preparation of ultrafine oxidized cellulose mats via electrospinning. *Biomacromol* 5:197–201. <https://doi.org/10.1021/bm034312g>
22. Zhang L, Li L, Wang L, Nie J, Ma G (2020) Multilayer electrospun nanofibrous membranes with antibacterial property for air filtration. *Appl Surf Sci* 515:145962. <https://doi.org/10.1016/j.apsusc.2020.145962>
23. Rethinam S, Basaran B, Vijayan S, Mert A, Bayraktar O, Aruni AW (2020) Electrospun nano-bio membrane for bone tissue engineering application- a new approach. *Mater Chem Phys* 249:123010. <https://doi.org/10.1016/j.matchemphys.2020.123010>
24. Zhu Y, Wu Y, Wang G, Wang Z, Tan Q, Zhao L, Wu D (2020) A flexible capacitive pressure sensor based on an electrospun polyimide nanofiber membrane. *Org Electron* 84:105759. <https://doi.org/10.1016/j.orgel.2020.1>
25. Shekh MI, Amirian J, Stadler FJ, Du B, Zhu Y (2020) Oxidized chitosan modified electrospun scaffolds for controllable release of acyclovir. *Int J Bio Macromol* 151:787–796. <https://doi.org/10.1016/j.ijbiomac.2020.02.230>
26. Wsoo MA, Shahir S, Bohari SPM, Nayan NHM, Razak SIA (2020) A review on the properties of electrospun cellulose acetate and its application in drug delivery systems: a new perspective. *Carbohydr Res* 491:107978. <https://doi.org/10.1016/j.carres.2020.107978>
27. Bhadra J, Parangusan H, Popelka A, Lehocky M, Humpolicek P, Al-Thania N (2020) Electrospun polystyrene/PANI-Ag fibers for organic dye removal and antibacterial application. *J Environ Chem Eng* 8:103746. <https://doi.org/10.1016/j.jece.2020.103746>
28. Zhang X, Huang Y, Zhou X, Wang F, Luo Z, Wu Q (2020) Characterizations of carbonized electrospun mats as diffusion layers for direct methanol fuel cells. *J Power Sources* 448:227410. <https://doi.org/10.1016/j.jpowsour.2019.227410>
29. Yin X, Zhang Z, Ma H, Venkateswaran S, Hsiao BS (2020) Ultra-fine electrospun nanofibrous membranes for multicomponent wastewater treatment: Filtration and adsorption. *Sep Purif Technol* 242:116794. <https://doi.org/10.1016/j.seppur.2020.116794>
30. Mukhiya T, Dahal B, Ojha GP, Chhetri K, Lee M, Kim T, Chae SH, Tiwari AP, Muthurasu A, Kim HY (2019) Silver nanoparticles entrapped cobalt oxide nanohairs/electrospun carbon nanofibers nanocomposite in apt architecture for high performance supercapacitors. *Compos B* 178:107482. <https://doi.org/10.1016/j.compositesb.2019.10>
31. Leyva BM, Felix FR, Chavez PT, Wong BR, Cervantes JL, Machado DS (2011) Preparation and characterization of durum wheat (triticum durum) straw cellulose nanofibers by electrospinning. *J Agric Food Chem* 59:870–875. <https://doi.org/10.1021/jf103364a>
32. Reddy N, Yang Y (2006) Properties of high-quality long natural cellulose fibers from rice straw. *J Agric Food Chem* 54:8081–8977. <https://doi.org/10.1021/jf0617723>
33. Costa SM, Mazzola PG, Silva JCAR, Pahl R, Pessoa A Jr, Costa SA (2013) Use of sugar cane straw as a source of cellulose for textile fiber production. *Ind Crops Prod* 42:189–194. <https://doi.org/10.1016/j.indcrop.2012.05.028>
34. Maheswari CU, Reddy KO, Muzenda E, Guduri BR, Rajulu AV (2012) Extraction and characterization of cellulose microfibrils from agricultural residue—*Cocos nucifera* L. *Biomass Bioenergy* 46:555–563. <https://doi.org/10.1016/j.biombioe.2012.06.039>
35. Li C, Chen R, Zhang X, Xiong J, Zheng Y, Dong W (2011) Fabrication and characterization of electrospun nanofibers of high DP natural cotton lines cellulose. *Fibers Polym* 12(3):345–351. <https://doi.org/10.1007/s12221-011-0345-4>
36. Haule LV, Carr CM, Rigout M (2016) Preparation and physical properties of regenerated cellulose fibres from cotton waste garments. *J Cleaner Prod* 112:4445–4451. <https://doi.org/10.1016/j.jclepro.2015.08.086>
37. Sjöholm E, Gustafsson K, Eriksson B, Brown W, Colmsjö A (2000) Aggregation of cellulose in lithium chloride/N,N-dimethylacetamide. *Carbohydr Polym* 41:153–161. [https://doi.org/10.1016/S0144-8617\(99\)00080-6](https://doi.org/10.1016/S0144-8617(99)00080-6)
38. Dupont AL (2003) Cellulose in lithium chloride/N,N-dimethylacetamide, optimisation of a dissolution method using paper substrates and stability of the solutions. *Polym* 44:4117–4126. [https://doi.org/10.1016/S0032-3861\(03\)00398-7](https://doi.org/10.1016/S0032-3861(03)00398-7)
39. Hamad AA, Hassouna MS, Shalaby TI, Elkady MF, Abd Elkawi MA, Hamad HA (2020) Electrospun cellulose acetate nanofiber incorporated with hydroxyapatite for removal of heavy metals. *Int J Biol Macromol* 151:1299–1313. <https://doi.org/10.1016/j.ijbiomac.2019.10.176>
40. Ojstrsek A, Fakin D, Hribernik S, Fakin T, Bracic M, Kurecic M (2020) Electrospun nanofibrous composites from cellulose acetate/ultra-high silica zeolites and their potential for VOC adsorption from air. *Carbohydr Polym* 236:116071. <https://doi.org/10.1016/j.carbpol.2020.116071>
41. Chen Y, Qiu LL, Ma XY, Dong LK, Jin ZF, Xia GB et al (2020) Electrospun cellulose polymer nanofiber membrane with flame resistance properties for lithium-ion batteries. *Carbohydr Polym* 234:115907. <https://doi.org/10.1016/j.carbpol.2020.115907>
42. Tanvir A, Ting VP, Eichhorn SJ (2020) Nanoporous electrospun cellulose acetate butyrate nanofibers for oil sorption. *Mater Lett* 261:127116. <https://doi.org/10.1016/j.matlet.2019.127116>
43. Zhu MN, Cao QP, Liu BY, Guo HY, Wang X, Han Y et al (2020) A novel cellulose acetate/poly (ionic liquid) composite air filter. *Cellulose* 27:3889–3902. <https://doi.org/10.1007/s10570-020-03034-8>
44. de Almeida DS, Duarte EH, Hashimoto EM, Turbiani FRB, Muniz EC, de Souza PR et al (2020) Development and characterization of electrospun cellulose acetate nanofibers modified by cationic

- surfactant. *Polym Test* 81:106206. <https://doi.org/10.1016/j.polymertesting.2019.106206>
45. Araga R, Sharma CS (2019) Amine functionalized electrospun cellulose nanofibers for fluoride adsorption from drinking water. *J Polym Environ* 27:816–826. <https://doi.org/10.1007/s10924-019-01394-2>
 46. Bacarin GB, Dognani G, dos Santos RJ, Meirelles MG, Rodrigues TF, Klauk CR et al (2020) Natural rubber composites with Grits waste from cellulose industry. *J Mater Cycles Waste Manage*. <https://doi.org/10.1007/s10163-020-01011-8> (Early Access-March 2020)
 47. Ishii D, Tatsumi D, Matsumoto T (2008) Effect of solvent exchange on the supramolecular structure, the molecular mobility and the dissolution behavior of cellulose in LiCl/DMAc. *Carbohydr Res* 343:919–928. <https://doi.org/10.1016/j.carres.2008.01.035>
 48. van de Ven T, Godbout L (2013) Cellulose fundamental aspects. Intech Open, Croatia (ISBN: 978-953-51-1183-2)
 49. Li B, Ding L, Xu HF, Mu XD, Wang HS (2017) Multivariate data analysis applied in alkali-based pretreatment of corn stover. *Resour Conserv Recycl* 122:307–318. <https://doi.org/10.1016/j.resconrec.2016.12.007>
 50. De Souza AG, Rocha DB, Kano FS, dos Santos RD (2019) Valorization of industrial paper waste by isolating cellulose nanostructures with different pretreatment methods. *Resour Conserv Recycl* 143:133–142. <https://doi.org/10.1016/j.resconrec.2018.12.031>
 51. Chen WF, Zhang SJ, He FF, Lu WP, Xv H (2019) Porosity and surface chemistry development and thermal degradation of textile waste jute during recycling as activated carbon. *J Mater Cycles Waste Manage* 21:315–325. <https://doi.org/10.1007/s10163-018-0792-8>
 52. Nowrouzi M, Behin J, Younesi H, Bahramifar N, Charpentier PA, Rohani S (2017) An enhanced counter-current approach towards activated carbon from waste tissue with zero liquid discharge. *Chem Eng J* 326:934–944. <https://doi.org/10.1016/j.cej.2017.05.141>
 53. Yousef S, Hamdy M, Tatarians M, Tuckute S, El-Abden SZ, Kliucininkas L, Baltusnikas A (2019) Sustainable industrial technology for recovery of cellulose from production waste and reprocessing into cellulose nanocrystals. *Resour Conserv Recycl* 149:510–520. <https://doi.org/10.1016/j.resconrec.2019.06.026>
 54. Chen R, Nie Y, Kato H, Wu J, Utashiro T, Lu J, Yue S, Jiang H, Zhang L, Li YY (2017) Methanogenic degradation of toilet-paper cellulose upon sewage treatment in an anaerobic membrane bioreactor at room temperature. *Bioresour Technol* 228:69–76. <https://doi.org/10.1016/j.biortech.2016.12.089>
 55. Son WK, Youk JH, Lee TS, Park WH (2004) Electrospinning of ultrafine cellulose acetate fibers: studies of a new solvent system and deacetylation of ultrafine cellulose acetate fibers. *J Polym Sci Part B Polym Phys* 42:5–11. <https://doi.org/10.1002/polb.10668>
 56. Kamide K (2005) Cellulose and cellulose derivatives—molecular characterization and its applications. Elsevier, New York (ISBN: 978-0-444-82254-3)
 57. Barhoum A, Makhoulf ASH (2018) Fundamentals of nanoparticles—classifications, synthesis methods, properties and characterization. Elsevier, Amsterdam (ISBN: 978-0-323-51255-8)
 58. Ramakrishna S, Fujihara K, Teo WE, Lim TC, Ma Z (2005) An introduction to electrospinning and nanofibers. World Scientific Publishing Co, Singapore (ISBN 981-256-425-2)
 59. Rosenau T, Potthast A, Hell J (2018) Cellulose science and technology—chemistry, analysis, and applications. Wiley, New Jersey
 60. Sukudom N, Jariyasakoolroj P, Jarupan L, Tansin K (2019) Mechanical, thermal, and biodegradation behaviors of poly(vinyl alcohol) biocomposite with reinforcement of oil palm frond fiber. *J Mater Cycles Waste Manage* 21:125–133. <https://doi.org/10.1007/s10163-018-0773-y>
 61. He X, Cheng L, Zhang X, Xiao Q, Zhang W, Lu C (2015) Tissue engineering scaffolds electrospun from cotton cellulose. *Carbohydr Polym* 115:485–493. <https://doi.org/10.1016/j.carbpol.2014.08.114>
 62. Ciolacu D, Ciolacu F, Popa V (2011) Amorphous cellulose—structure and characterization. *Cellul Chem Technol* 45:13–21
 63. Kargazadeh H, Sheltami RM, Ahmad I, Abdullah I, Dufresne A (2015) Cellulose nanocrystal: a promising toughening agent for unsaturated polyester nanocomposite. *Polym* 56:346–357. <https://doi.org/10.1016/j.polymer.2014.11.054>
 64. Park YB, Lee CM, Koo BW, Park S, Cosgrove DJ, Kim SH (2013) Monitoring meso-scale ordering of cellulose in intact plant cell walls using sum frequency generation spectroscopy. *Plant Physiol* 163:907–913. <https://doi.org/10.1104/pp.113.225235>
 65. Regiani AM, Frollini E, Marson GA, Arantes GM, El Seoud OA (1999) Some aspects of acylation of cellulose under homogeneous solution conditions. *J Polym Sci Part A Polym Chem* 37:1357–1363
 66. Zhao YY, Yang QB, Lu XF, Wang C, Wei Y (2005) Study on correlation of morphology of electrospun products of polyacrylamide with ultrahigh molecular weight. *J Polym Sci* 43:2190–2195. <https://doi.org/10.1002/polb.20506>
 67. Lee KH, Kim HY, Bang HJ, Jung YH, Lee SG (2003) The change of bead morphology formed on electrospun polystyrene fibers. *Polymers* 44:4029–4034. [https://doi.org/10.1016/S0032-3861\(03\)00345-8](https://doi.org/10.1016/S0032-3861(03)00345-8)
 68. Fong H, Chun I, Reneker DH (1999) Beaded nanofibers formed during electrospinning. *Polymers* 40:4585–4592. [https://doi.org/10.1016/S0032-3861\(99\)00068-3](https://doi.org/10.1016/S0032-3861(99)00068-3)
 69. Zhao H, Chi H (2018) Electrospun bead-on-string fibers: useless or something of value? In: Lin T (ed) Novel aspects of nanofibers. Intechopen limited, London, p 87
 70. Langer R (2000) Biomaterials in drug delivery and tissue engineering: one laboratory's experience. *Acc Chem Res* 33:94–101. <https://doi.org/10.1021/ar9800993>
 71. Kaur S, Sundarajan S, Rana D, Matsuura T, Ramakrishna S (2012) Influence of electrospun fiber size on the separation efficiency of thin film nanofiltration composite membrane. *J Membr Sci* 392:101–111. <https://doi.org/10.1016/j.memsci.2011.12.005>
 72. Yun K, Hogan C, Matsubayashi Y, Kawabe M, Iskandar F, Okuyama K (2007) Nanoparticle filtration by electrospun polymer fibers. *Chem Eng Sci* 62:4751–4759. <https://doi.org/10.1016/j.ces.2007.06.007>
 73. Xue MQ, Li FW, Wang Y, Cai XJ, Pan F, Chen JT (2013) Ultralow-limit gas detection in nano-dumbbell polymer sensor via electrospinning. *Nanoscale* 5:1803–1805. <https://doi.org/10.1039/c3nr34090b>

Publisher's Note Springer Nature remains neutral with regard to jurisdictional claims in published maps and institutional affiliations.